Antisense RNA-mediated transcriptional attenuation in plasmid pIP501: the simultaneous interaction between two complementary loop pairs is required for efficient inhibition by the antisense RNA

Nadja Heidrich and Sabine Brantl

Friedrich-Schiller-Universität Jena, AG Bakteriengenetik, Philosophenweg 12, D-07743 Jena, Germany

Correspondence
Sabine Brantl
Sabine.Brantl@uni-jena.de

Received 12 September 2006
Revised 2 November 2006
Accepted 14 November 2006

Streptococcal plasmid pIP501 uses antisense RNA-mediated transcriptional attenuation to regulate its replication. Previous *in vitro* assays suggested that binding intermediates between RNAII (sense RNA) and RNAIII (antisense RNA) are sufficient for inhibition, and a U-turn structure on RNAII loop L1 was found to be crucial for the interaction with RNAIII. Here, sequence and structural requirements for an efficient RNAII–RNAIII interaction were investigated. A detailed probing of RNA secondary structure combined with *in vitro* single-round transcription assays indicated that complex formation between the two molecules progresses into the lower stems of both loop pairs of the sense and antisense RNAs, but that the complex between RNAII and RNAIII is not a full duplex. Stem–loops L3 and L4 were required to be linked to one other for efficient contact with the complementary loops L2 and L1 of the sense RNA, indicating a simultaneous interaction between these two loop pairs. Thereby, the sequence and length of the spacer connecting L3 and L4 were shown not to be important for inhibition.

INTRODUCTION

Antisense RNA-mediated gene regulation has been found and studied in prokaryotic accessory DNA elements such as plasmids, phages and transposons, and a broad variety of regulatory mechanisms has been observed (reviewed by Brantl, 2004). During the past 5 years, a growing number of recently identified chromosomally encoded small RNAs have been included in such studies (e.g. Zhang *et al.*, 2002; Rasmussen *et al.*, 2005; Udekwu *et al.*, 2005). Independently of whether binding initiates by loop–loop contacts (plasmid copy number control systems) or linear region–loop contacts (e.g. hok/sok of plasmid R1; Thisted *et al.*, 1994), a rapid interaction between antisense and target RNA has been shown to be crucial for regulation (reviewed by Wagner *et al.*, 2002). Structural requirements for efficient antisense RNAs have been defined (Hjalt & Wagner, 1992, 1995) and pairing rate constants for sense/antisense RNA pairs calculated to be mainly in the range of $10^6\ \mathrm{M}^{-1}\ \mathrm{s}^{-1}$. Only for a few plasmid-encoded antisense RNA systems has a detailed biochemical analysis been performed to investigate the structural and sequence requirements for inhibition (e.g. Asano & Mizobuchi, 2000; Greenfield *et al.*, 2001). For CopA (antisense RNA) of plasmid R1, the multistep pathway of interaction with its sense RNA (CopT) has been elucidated in detail, and a four-helix junction has been identified as the inhibitory intermediate (Kolb *et al.*, 2000a, b). A subsequent study on Inc RNA/*repZ* mRNA of Col1b-P9 suggests that similar pathways are used to form inhibitory antisense–target RNA complexes (Kolb *et al.*, 2001). Apparently, in many cases, kissing is sufficient for inhibition, and inhibitory intermediates as in R1 are only slowly converted into full duplexes (Wagner & Brantl, 1998; Malmgren *et al.*, 1997).

Streptococcal plasmid pIP501 exerts its replication control by the concerted action of a small antisense RNA (RNAIII, 136 nt) and a transcriptional repressor, CopR (Brantl & Behnke, 1992). The deletion of either control component causes a 10- to 20-fold increase in plasmid copy number; a simultaneous deletion has, however, no additive effect. RNAIII functions by transcriptional attenuation of the *repR* mRNA (RNAII) that encodes the rate-limiting replication initiator protein (Brantl *et al.*, 1993). CopR acts as a transcriptional repressor at the essential *repR* promoter (Brantl, 1994). Additionally, it has a second function: since RNAIII, with an half-life of ~30 min, is unusually stable (Brantl & Wagner, 1996), it would not be able to correct downward fluctuations in copy number. Therefore, CopR is

---

Abbreviations: CMCT, 1-cyclohexyl-3(2-morpholinoethyl) carbodiimide metho-*p*-toluenesulfonate; RT, reverse transcription.

2006/002329

required to prevent convergent transcription from the sense promoter pII and the antisense promoter pIII, thereby indirectly increasing the amount of RNAIII (Brantl, 1994; Brantl & Wagner, 1997). When copy number decreases, decreased CopR synthesis will derepress pII. This results in increased transcription of RNAII and convergent transcription, which decreases transcription of RNAIII. Both effects increase RepR synthesis and, consequently, the replication frequency. Fig. 4(A) presents a model of replication control of pIP501.

In vitro assays show that RNAIII-mediated inhibition occurs faster than complete duplex formation, suggesting that binding intermediates between RNAII and RNAIII are sufficient for inhibition (Brantl & Wagner, 1994). Furthermore, the deletion of stem–loops L1 and L2 at the 5′ end of RNAIII has no effect on the inhibitory function of RNAIII *in vivo* (Brantl *et al.*, 1993), whereas mutations in loop L3 of RNAIII lead to new incompatibility groups (Brantl & Wagner, 1996), indicating that L3 is the recognition loop. However, since a U-turn structure on loop L1 of RNAII complementary to L4 of RNAIII proves to be important for an efficient interaction with RNAIII, we have suggested that L3 and L4 are of equal importance for the initial contact (Heidrich & Brantl, 2003).

Here, we investigate the sequence and structural requirements for an efficient RNAII–RNAIII interaction of plasmid pIP501 by a combination of secondary-structure probing and attenuation assays with wild-type and mutated RNAIII species, as well as single stem–loops. Our results demonstrate that helix formation progresses into the lower parts of stems L3 and L4, whereas the 6 nt spacer separating them remains unpaired. The sequence and length of this spacer are not important for efficient inhibition, and the exclusive function of the spacer is to present both stem–loops simultaneously for interaction with the complementary loop pair L1/L2 of RNAII.

METHODS

Enzymes and chemicals. Chemicals used were of the highest purity available. T7 RNA polymerase and T4 polynucleotide kinase were purchased from NEB, Firepol Taq polymerase from Solis Biodyne, and Thermoscript reverse transcriptase from Invitrogen. *Bacillus subtilis* RNA polymerase was prepared by J. M. Sogo, Universidad Autónoma de Madrid. 1-Cyclohexyl-3(2-morpholinoethyl) carbodiimide metho-*p*-toluenesulfonate (CMCT) and lead acetate from Merck, and DMSO from Fluka, were used for the chemical probing.

In vitro transcription. *In vitro* transcription experiments were performed as described previously (Brantl & Wagner, 1996; Heidrich & Brantl, 2003). Templates for *in vitro* transcription of mutated RNAIII species were generated by PCR on plasmid pPR1 as template (Brantl & Behnke, 1992), with oligonucleotide SB1 (Brantl & Wagner, 1994) and one of the following mutagenic oligodeoxyribonucleotides:

SB547: 5′ TTA ATT GAT TGG TGG TAA TCA ATT AAC CGA TAC AGT TAA AGT TTC TCA GGC TTT AAC TGG TCG TGG CTC TT 3′

SB548: 5′ TTA ATT GAT TGG TGG TAA TCA ATT AAG CGC AGT TAA AGT TTC TCA GGC TTT AAC TGG TCG TGG CTC TT 3′

SB 570: 5′ TTA ATT GAT TGG TGG TAA TCA ATT AAC AGT TAA AGT TTC TCA GGC TTT AAC TGG TCG TGG CTC TT 3′

SB571: 5′ TTA ATT GAT TGG TGG TAA TCA ATT AAG GCT CGA CAC GGC AGT TAA AGT TTC TCA GGC TTT AAC TGG TCG TGG CTC TT 3′

SB619: 5′ AAT ATT GAT TGG TGG TAA TCA ATA TTG GCT CGG TCT TAA AGT TTC TCA GGC TTT AAG ACG TCG TGG CTC TT 3′

SB620: 5′ AAT TTT GAT TGG TGG TAA TCA AAA TTG GCT CGG TCA TAA AGT TTC TCA GGC TTT ATG ACG TCG TGG CTC TT 3′

SB645: 5′ AAT TTT GAT TGG TGG TAA TCA AAA TTG GCT CGC AGT TAA AGT TTC TCA GGC TTT AAC TGG TCG TGG CTC TT 3′

The template for RNAIII$_{72}$ was generated as described previously (Brantl & Wagner, 1994).

The template fragment for RNAII complementary to SB645 was generated by a two-step PCR on pPR1 as template, with outer primers SB6 and SB7 (Brantl & Wagner, 1994) and the following mutagenic oligonucleotides as inner primers:

SB646: 5′ TTT AAC TGC GAG CCA ATT TTG ATT ACC ACC AAT CAA AAT TAG AAG TCG AGA CCC 3′

SB647: 5′ GGG TCT CGA CTT CTA ATT TTG ATT GGT GGT AAT CAA AAT TGG CTC GCA GTT AAA 3′

Loops L3 and L4 of RNAIII were synthesized *in vitro* and consisted of the following sequences:

L3: 5′ AAU UGA UUG GUG GUA AUC AAU U 3′

L4: 5′ GUU AAA GUU UCU CAG GCU UUA AC 3′

Secondary structure analysis. Secondary-structure probing with chemical probes (Pb^{2+}, CMCT and DMSO) using 2 pmol of unlabelled RNAIII in a total volume of 20 µl was carried out according to Brunel & Romby, 2000, as follows. Reaction buffers of the following final concentrations were used: for CMCT, 25 mM borate-NaOH, pH 8.0, 5 mM magnesium acetate, 75 mM potassium acetate, 5 mM β-mercaptoethanol; for DMSO, 25 mM Tris/HCl, pH 7.5, 5 mM MgCl$_2$, 75 mM KCl, 5 mM β-mercaptoethanol; for Pb^{2+}, 25 mM Tris-acetate, pH 7.5, 5 mM magnesium acetate, 25 mM sodium acetate. Denaturing buffers were: for CMCT, 25 mM borate-NaOH, 1 mM EDTA; for DMSO, 25 mM Tris/HCl, pH 7.5, 1 mM EDTA. RNA-removal buffers for the CMCT and DMSO reactions contained 10 mM Tris/HCl, pH 7.5, 1.5 mM EDTA and 0.1 % SDS. A subsequent reverse-transcription (RT) reaction was used to visualize the products. Primer hybridization was done in a total volume of 12 µl containing 9 µl of the modified RNA, 1 µl with 100 000 c.p.m. of 5′ [^{32}P]-labelled oligonucleotide SB2 (Hartmann Analytic) (Brantl & Wagner, 1994) and 2 µl 10 mM dNTPs for 5 min at 65 °C, followed by RT with ThermoScript reverse transcriptase (2 U, Invitrogen) in 20 µl for 45 min at 55 °C. Partial digestions of *in vitro*-synthesized, unlabelled RNAIII and RNAII species with ribonucleases T1, T2 and V were performed in the same way as those described previously for 5′ end-labelled species (Heidrich & Brantl, 2003), except that digestions were followed by an RT reaction with 5′ end-labelled primer SB2 (see above). All reaction products were subjected to electrophoresis in 8 % denaturing polyacrylamide gels.

Single-round transcription assays and calculation of inhibition rate constant k_{inhib}. Single-round transcription assays were performed as described previously (Brantl & Wagner, 1994), using PCR-generated 500 bp DNA fragments of pPR1 (comprising promoters p_{II} and p_{III}, the attenuator and 100 bp downstream) as templates and *B. subtilis* RNA polymerase prepared by J. M. Sogo. The protocol of the attenuation experiments was as described previously (Brantl & Wagner, 1994), with one alteration: the concentration of the unlabelled RNAIII species included was determined by UV spectrophotometry. The inhibition rate constants were calculated as described previously (Brantl & Wagner, 1994).

RESULTS AND DISCUSSION

Pairing between RNAII and RNAIII does not yield a full duplex

Previously, the secondary structures of RNAIII and RNAII were probed with RNases T1 (single-stranded Gs), T2 (single-stranded region with a slight preference for As) and V (double-stranded and stacked regions) (Brantl & Wagner, 1994). To obtain more detailed information about the 3′

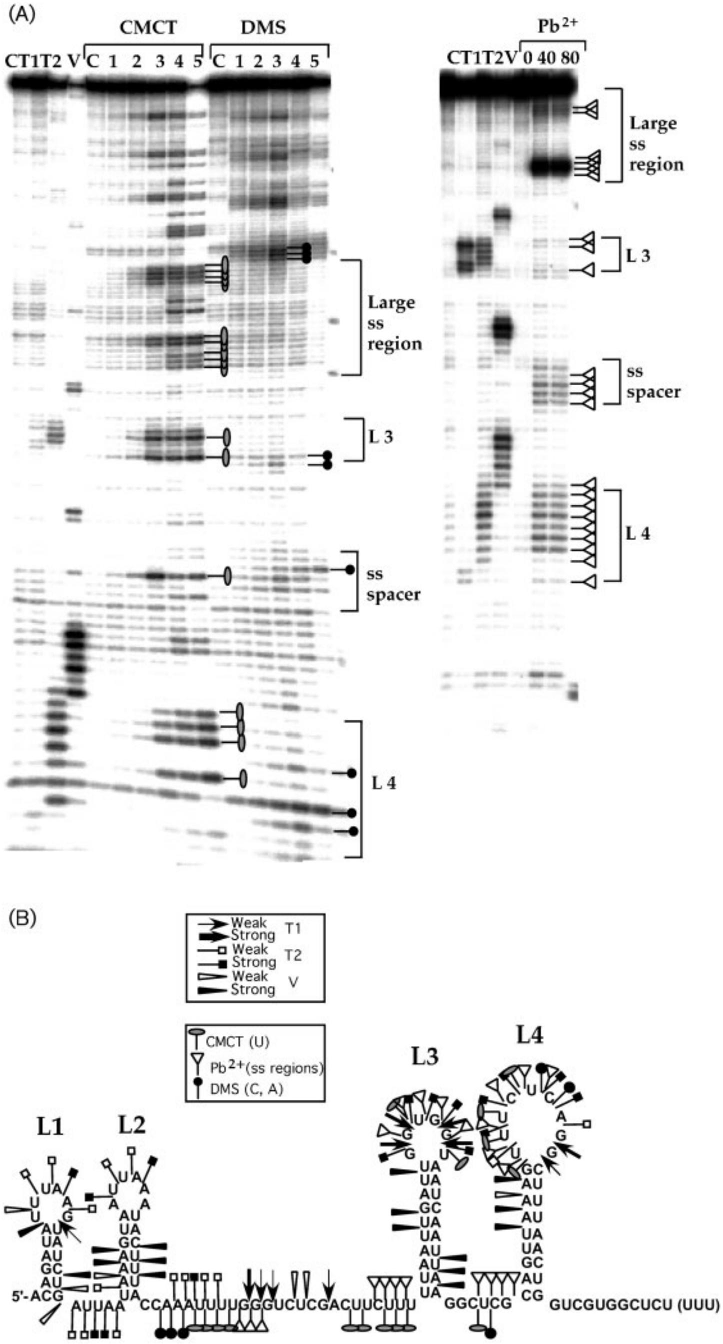

Fig. 1. Fine mapping of the secondary structure of RNAIII by a combination of enzymic and chemical probes. A secondary-structure probing of wild-type RNAIII$_{136}$ with three different RNases and chemical probes is shown. Purified, unlabelled RNA species were subjected to limited cleavage with RNases T1, T2 or V, or alternatively treated with CMCT, DMSO or Pb^{2+}, as indicated, and afterwards subjected to an RT reaction with 5′ end-labelled primer SB2, as described in Methods. The reaction products were separated on 8 % denaturing gels. (A) PhosphorImager prints. The RNase concentrations used were: T1, 10^{-2} U μl^{-1}; T2, 10^{-1} U μl^{-1}; V, 10^{-1} U ml^{-1}. C, control without RNases. Concentrations used for CMCT were: 5 mM (lane 1), 10 mM (lanes 2 and 4) and 25 mM (lanes 3 and 5); for DMSO, 50 mM (lane 1), 100 mM (lanes 2 and 4) and 200 mM (lanes 3 and 5). For both CMCT and DMSO, lanes 4 and 5 show treatment under denaturing conditions. For Pb^{2+} treatment, concentrations of 40 and 80 mM were used. Signals obtained with the chemical probes are indicated in the autoradiograms of the corresponding gels and explained in the key in (B). Brackets denote loops L3 and L4, the single-stranded (ss) spacer between these loops and the large single-stranded region 5′ of L3. (B) Secondary structure of RNAIII$_{136}$ based on the cleavage data and additional experiments (not shown). The keys show the symbols used to designate contacts obtained by enzymic or chemical probing.

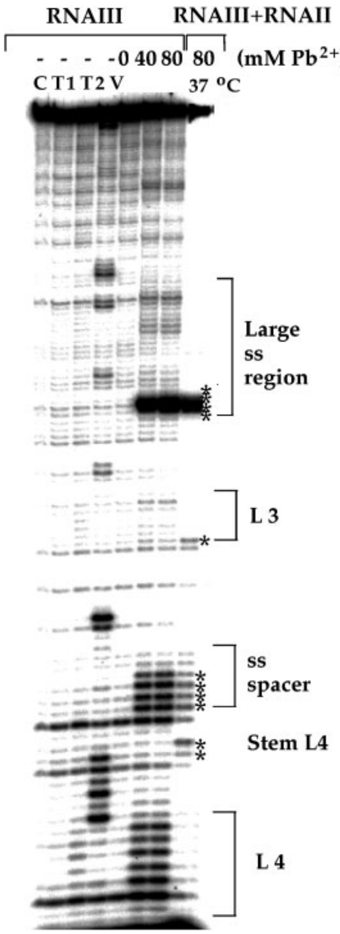

Fig. 2. Pb^{2+} probing of RNAIII and the RNAIII–RNAII complex. Purified, unlabelled RNAIII (0.5 pmol) was incubated with unlabelled RNAII (5 pmol), and the complex was allowed to form for 5 min at 37 °C and subjected to cleavage with Pb^{2+} followed by an RT reaction with 5′ end-labelled primer SB2, as described in Methods. In parallel, unlabelled RNAIII alone was subjected to cleavage with the RNases T1, T2 and V, or with 40 and 80 mM Pb^{2+}, and the products subjected to an RT reaction with labelled primer SB2. The reaction products were separated on 8 % denaturing gels. An autoradiogram is shown. RNase concentrations used were as in Fig. 1. C, control without RNase treatment. Asterisks denote the alteration of the Pb^{2+} cleavage pattern upon pairing. Brackets indicate loops L3 and L4, the single-stranded (ss) spacer between these loops and the large single-stranded region 5′ of L3.

stem–loops L3 and L4 and the spacer in between them, additional structure-probing experiments were performed with CMCT (Us), Pb^{2+} (single-stranded regions) and DMSO (Cs and As), as described in Methods. The results are shown in Fig. 1. Four cuts for Pb^{2+} and one cut each for DMSO and CMCT within the spacer region, as well as three cuts for V in the lower stem of L3, confirmed that the spacer between L3 and L4 is indeed 6 nt long. Furthermore, the sizes of L3 with 6 nt and of L4 with 9 nt as well as that of the large single-stranded region 5′ of stem–loop L3 were corroborated by a combination of enzymic and chemical probing.

Since Pb^{2+} is a sensitive probe for single-stranded sequences, it was used to probe the structure of a complex between the 5′ 184 nt of RNAII (containing the target for RNAIII) and 5′-labelled full-length RNAIII$_{136}$. For comparison, unpaired RNAIII was probed with T1, T2, V and Pb^{2+}. As shown in Fig. 2, cleavage positions indicated that the RNAII–RNAIII complex is not fully base-paired in the single-stranded region between L3 and L4 of RNAIII. Four significant Pb^{2+} cuts within the large single-stranded region 5′ of L3 that were not reduced upon pairing with RNAII suggested that at least part of this region also remained single stranded. By contrast, the loops were found to be almost completely paired, with the exception of the 3′ outermost U of L3. Interestingly, 2 nt of the 5′ half of stem L4 became single stranded (asterisks in Fig. 2). Lead cleavage cannot be used to assess whether the stems of L3/L2 and L4/L1 are engaged in intramolecular or intermolecular helices.

To answer this question and to evaluate the role of the spacer region between L3 and L4, single-round transcription experiments were performed to determine the inhibition rate constants of mutated antisense RNAs with either wild-type or complementary sense RNAs. In all these experiments, RNAIII$_{72}$, consisting only of stem–loops L3 and L4 with their 6 bp spacer region, was used as a 'wild-type' species, since previous experiments had shown that inhibition does not require stem–loops L1 and L2 and the large single-stranded region (Brantl & Wagner, 1994).

The stems are involved in the formation of intermolecular helices

In RNAIII of pIP501, the stems of L3 and L4 consist of only 10 and 9 bp, respectively, and are not interrupted by bulges that, in longer helices, protect the antisense RNAs against degradation by RNase III and are required for efficient strand opening (Hjalt & Wagner, 1995). To find out whether pairing is restricted to the 6 and 9 nt loops L3 and L4, respectively, mutated RNAIII species with 3 or 4 bp heterologous stem bases of L3 and L4 were assayed in single-round transcription experiments (Fig. 3A). Whereas a heterologous 3 bp stem base in L3 and L4 yielded twofold lower inhibition rate constants (RNAIII$_{619}$), an extension to 4 heterologous bp in L3 and L4 reduced k_{inhib} fourfold (RNAIII$_{620}$). The reduced inhibition rate constants with wild-type RNAII could, at least partially, be compensated when a complementary mutated RNAII was used. This was shown with RNAIII$_{645}$, which contained a heterologous 4 bp stem base in L3 alone. These data (summarized in Table 1) demonstrate that in the inhibitory complex, pairing progresses into the lower part of stems L3 and L4 of RNAIII, and that the stems are involved in the formation of intermolecular helices with the sense RNA (RNAII). A recent analysis of the FinP/*traJ* system of the F plasmid that acts by inhibition of *traJ* translation has also revealed that base pairing proceeds from an initial loop–loop interaction

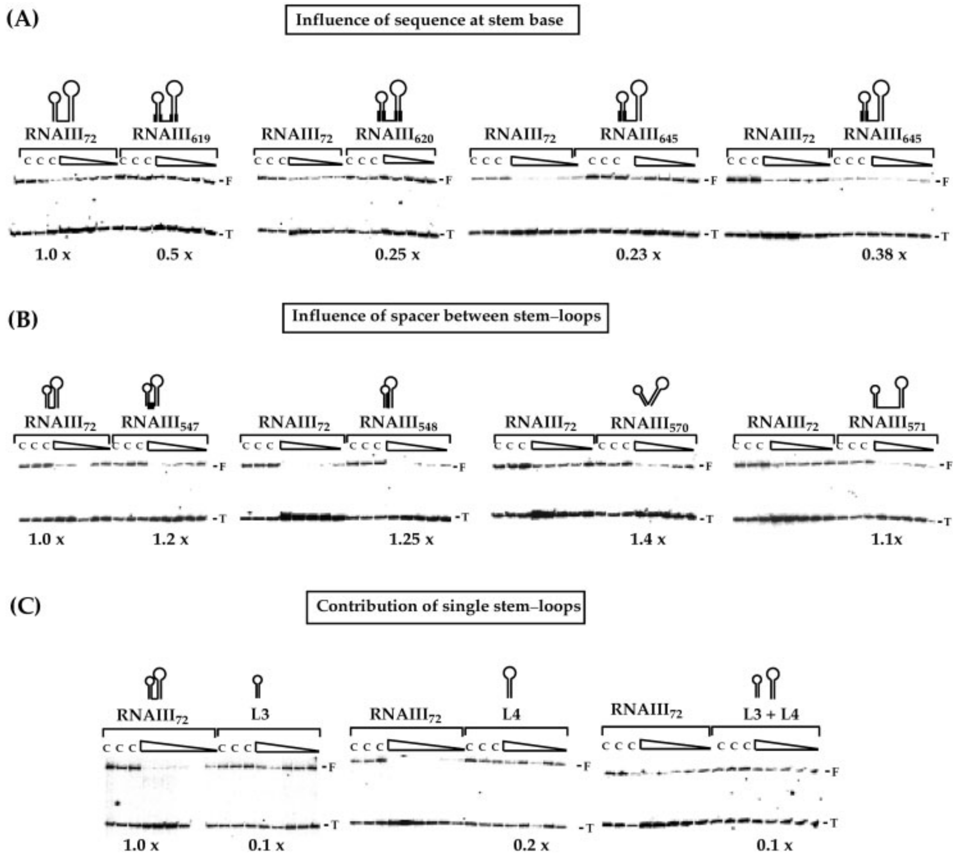

Fig. 3. Single-round transcription assays with wild-type and mutated RNAIII species. *In vitro* attenuation assays were performed with wild-type RNAIII$_{72}$ containing stem–loops L3 and L4 and a series of truncated and mutated RNAIII species. RNAIII species were incorporated at different concentrations (1.0, 0.6, 0.4, 0.2, 0.1 and 0.05×10^{-7} M for RNAIII$_{72}$, and 1.0, 0.6, 0.4, 0.2 and 0.1×10^{-7} M for the mutated species), denoted by a triangle, and their effects on induced transcription termination were determined at a 10 min time point. The figure shows PhosphorImager prints with the positions of full-length run-off *repR*-RNA (~365 nt, F) and terminated *repR*-RNA (~260 nt, T). Calculation of band intensity, background substraction and calculation of the inhibition rate constant k_{inhib} were performed as described previously (Brantl & Wagner, 1994; Heidrich & Brantl, 2003). Three buffer controls (C) show the value in the absence of antisense RNA. The mean intensity of the F band in the buffer controls was set to 100 % (regulatable F). Below the gels, the relative inhibition rate constants k_{inhib} are shown. The calculated k_{inhib} values and the mutations present in the different RNAIII species are summarized in Table 1. (A) Influence of the sequence at the stem base; (B) influence of the spacer between the stem–loops; (C) contribution of single stem–loops.

through the top portion of the stems to a stable duplex (Gubbins *et al.*, 2003). By contrast, in the inhibitory intermediate of CopA and CopT of plasmid R1, only the upper parts of the stems of the decisive 3′ CopA stem–loop pair containing a bulge region are involved in intermolecular helices, whereas the lower parts remain paired intramolecularly (Kolb *et al.*, 2000a).

The sequence and length of the spacer between L4 and L3 do not affect the inhibitory function of RNAIII

In sense–antisense systems containing two complementary loop pairs, the length of the spacer between the two stem–loops is found to be different (for examples, see Brantl, 2004). To analyse the influence of the length and sequence of the spacer between L3 and L4, mutated RNAIII species with varying spacer lengths and with a heterologous spacer were investigated in the attenuation assay. As shown in Fig. 3(B), RNAIII$_{547}$, which contains a heterologous spacer, was slightly more inhibitory than the wild-type, indicating that the sequence of the spacer is not important. This corresponds well with the results of the Pb^{++}-based secondary-structure probing of the RNAII–RNAIII complex, in which this spacer was still lead sensitive, i.e. single stranded, although the loops were almost completely paired (Fig. 2). Both RNAIII$_{548}$ with a 3 nt spacer and RNAIII$_{571}$ with a 12 nt spacer were as efficient in inhibition

Table 1. Inhibition rate constants of wild-type and mutated RNAIII species

Values represent the means of at least three independent determinations. The inhibition rate constant for RNA$_{72}$ is the mean of 33 independent determinations.

RNA species	Characteristics	Inhibition rate constant k_{inhib} ($M^{-1}\ s^{-1}$)	Relative k_{inhib}
RNA$_{619}$	Heterologous 3 bp stem base in L3/L4	0.75×10^6	0.5
RNA$_{620}$	Heterologous 4 bp stem base in L3/L4	0.4×10^6	0.25
RNA$_{645}$	Heterologous 4 bp stem base in L3 wild-type template	0.37×10^6	0.23
RNA$_{645}$	Heterologous 4 bp stem base in L3 complementary template	0.6×10^6	0.38
RNA$_{547}$	Heterologous 6 nt spacer	1.9×10^6	1.2
RNA$_{548}$	3 nt spacer	2.0×10^6	1.25
RNA$_{570}$	No spacer between L3 and L4	2.2×10^6	1.4
RNA$_{571}$	12 nt spacer	1.8×10^6	1.1
RNAIII$_{72}$	Wild-type L3 and L4, 6 bp spacer	1.6×10^6	1
Stem–loop L3	Synthetic RNA oligonucleotide	1.4×10^5	0.1
Stem–loop L4	Synthetic RNA oligonucleotide	3.0×10^5	0.2
Stem–loops L3 + L4	Mixed 1 : 1	1.25×10^5	0.1

as the wild-type with a 6 nt spacer, suggesting that the spacer length can be varied. Interestingly, RNAIII$_{570}$, which does not contain a spacer between L3 and L4, exhibited an increase of 1.4-fold in k_{inhib} compared with the wild-type. These results prove unequivocally that neither the sequence nor the length of the spacer between L3 and L4 influences the inhibitory function of RNAIII.

A simultaneous interaction between both loop pairs of RNAII and RNAIII is required for inhibition

Based on the results with the spacer mutants, we asked whether a mixture of the unlinked stem–loops L3 and L4 is efficient in inhibition. For this purpose, synthetic RNA

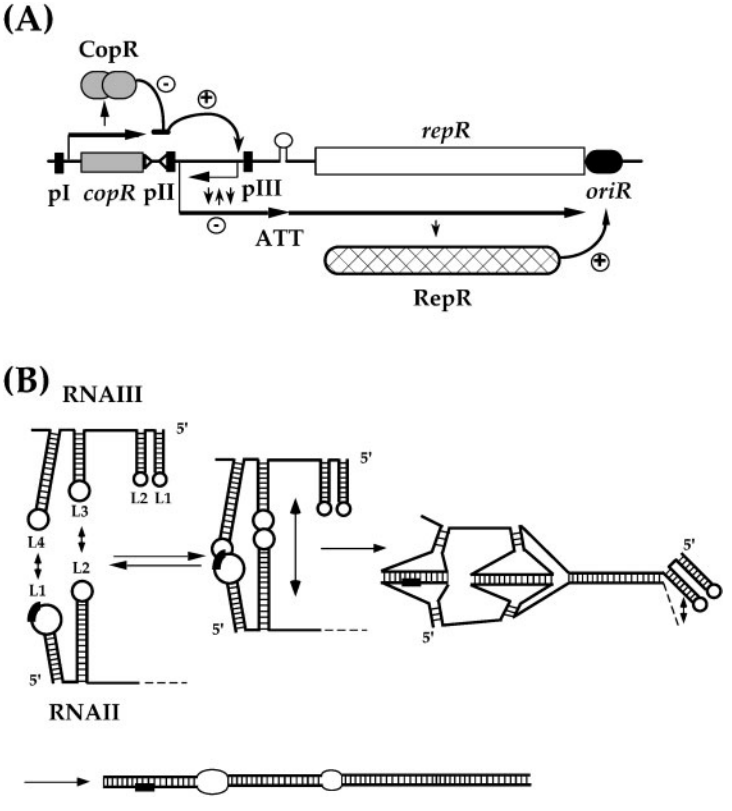

Fig. 4. Model for the interaction between RNAIII and RNAII in the context of replication control of plasmid pIP501. (A) Working model of copy number control of plasmid pIP501 in *B. subtilis*. Black boxes, promoters; rectangles, ORFs; thick arrows, RNAs; grey/stippled, proteins; *oriR*, replication origin; stem–loop/ATT, transcriptional attenuator (rho-independent terminator); +, activation; −, repression/inhibition. (B) Putative binding pathway of RNAII and RNAIII of pIP501. A putative RNAIII–RNAII binding pathway was derived from the experimental data presented in Figs 1–3. First, loop pairs L1 (U-turn motif highlighted in black)/L4 and L2/L3 interact simultaneously. Subsequently, basepairing is extended into the lower stem regions, and the large spacer region of RNAIII comes into contact with the complementary region in RNAII. Finally, only the spacer separating L3 and L4 in RNAIII and L1 and L2 in RNAII, as well as the 5′ 4 nt of the large single-stranded region 5′ of L3, remain single-stranded.

oligonucleotides containing either L3 or L4 were used. First, each stem–loop was investigated separately in the attenuation assay (Fig. 3C). As expected, L3 and L4 alone were 10-fold and fivefold less efficient, respectively, than RNAIII$_{72}$. This is in good correlation with the previous result, whereby a less than 0.1-fold inhibitory activity was found for RNAIII$_{47}$ containing only the large single-stranded region and L3 (Brantl & Wagner, 1994). Surprisingly, a 1 : 1 mixture of L3 and L4 was as inefficient in inhibition as L3 alone. Therefore, we can conclude that L3 and L4 have to be attached to one other to ensure efficient inhibition. Apparently, this function is provided by the 6 nt spacer in wild-type RNAIII, which acts as a scaffold for both stem–loops. Consequently, a simultaneous interaction between the two loop pairs of RNAIII and RNAII is required for transcriptional attenuation to occur. This finding is in accordance with our previous result that L4, which is complementary to U-turn loop L1 of RNAII, is important for an efficient contact with the sense RNA (Heidrich & Brantl, 2003). Fig. 4(B) relates the results of this study to the working model of copy-number control. A requirement for both stem–loops of the antisense RNA (RNAI) for efficient complex formation with the sense RNA, *repC* mRNA, was also found in an *in vitro* study of the transcription attenuation system of staphylococcal plasmid pT181. Here, two antisense RNAs, RNAI$_{84}$ (stem loops L1 and L2 connected by an 8 nt spacer) and RNAI$_{146}$ (stem–loops L1 to L 4) are expressed *in vivo* that bound equally well to *repC* mRNA. However, upon deletion of either L1 or L2 or the 3′ part of L2, pairing was reduced 10- to 100-fold (Brantl & Wagner, 2000). By contrast, in plasmid R1, the initial contact with the target RNA is made by the 3′ stem–loop of the antisense RNA CopA, and the 5′ stem–loop is only involved in later pairing intermediates (see Kolb *et al.*, 2000a).

The recently found chromosomally encoded bona fide antisense regulators belong mainly to the trans-encoded RNAs that are only partially complementary to their targets. However, searches for cis-encoded antisense RNAs from different bacterial genomes are under way, and it remains to be seen how new results for such RNAs will expand our knowledge of RNA–RNA interactions involved in prokaryotic gene regulation.

ACKNOWLEDGEMENTS

We acknowledge E. Birch-Hirschfeld (Institute for Virology, Jena) for synthesizing various oligodeoxyribonucleotides, and Margarita Salas and J. M. Sogo, Universidad Autónoma de Madrid, for providing us with purified *B. subtilis* RNA polymerase. This work was supported by grant BR 1552/4-4 from the Deutsche Forschungsgemeinschaft (to S. B.).

REFERENCES

Asano, K. & Mizobuchi, K. (2000). Structural analysis of late intermediate complex formed between plasmid ColIb-P9 Inc RNA and its target RNA. How does a single antisense RNA repress translation of two genes at different rates? *J Biol Chem* **275**, 1269–1274.

Brantl, S. (1994). The *copR* gene product of plasmid pIP501 acts as a transcriptional repressor at the essential *repR* promoter. *Mol Microbiol* **14**, 473–483.

Brantl, S. (2004). Plasmid replication controlled by antisense RNAs. In *The Biology of Plasmids*, chapter 3, pp. 47–62. Edited by B. Funnell & G. Phillips. Washington, DC: AMS Press.

Brantl, S. & Behnke, D. (1992). Copy number control of the streptococcal plasmid pIP501 occurs at three levels. *Nucleic Acids Res* **20**, 395–400.

Brantl, S. & Wagner, E. G. H. (1994). Antisense RNA-mediated transcriptional attenuation occurs faster than stable antisense/target RNA pairing: an *in vitro* study of plasmid pIP501. *EMBO J* **13**, 3599–3607.

Brantl, S. & Wagner, E. G. H. (1996). An unusually long-lived antisense RNA in plasmid copy number control: *in vivo* RNAs encoded by the streptococcal plasmid pIP501. *J Mol Biol* **255**, 275–288.

Brantl, S. & Wagner, E. G. H. (1997). Dual function of the *copR* gene product of plasmid pIP501. *J Bacteriol* **179**, 7016–7024.

Brantl, S. & Wagner, E. G. H. (2000). Antisense RNA-mediated transcriptional attenuation: an *in vitro* study of plasmid pT181. *Mol Microbiol* **35**, 1469–1482.

Brantl, S., Birch-Hirschfeld, E. & Behnke, D. (1993). RepR protein expression on plasmid pIP501 is controlled by an antisense RNA-mediated transcription attenuation mechanism. *J Bacteriol* **175**, 4052–4061.

Brunel, C. & Romby, P. (2000). Probing RNA structure in solution. *Methods Enzymol* **318**, 3–21.

Greenfield, T. J., Franch, T., Gerdes, K. & Weaver, K. E. (2001). Antisense RNA regulation of the *par* post-segregational killing system: structural analysis and mechanism of binding of the antisense RNA, RNAII and its target, RNAI. *Mol Microbiol* **42**, 527–537.

Gubbins, M. J., Arthur, D. C., Ghetu, A. F., Glover, J. N. M. & Frost, L. S. (2003). Characterizing the structural features of RNA/RNA interactions of the F-plasmid FinOP fertility inhibition system. *J Biol Chem* **278**, 27663–27671.

Heidrich, N. & Brantl, S. (2003). Antisense-RNA mediated transcriptional attenuation: importance of a U-turn loop structure in the target RNA of plasmid pIP501 for efficient inhibition by the antisense RNA. *J Mol Biol* **333**, 917–929.

Hjalt, T. & Wagner, E. G. H. (1992). The effect of loop size in antisense and target RNAs on the efficiency of antisense RNA control. *Nucleic Acids Res* **20**, 6723–6732.

Hjalt, T. & Wagner, E. G. H. (1995). Bulged-out nucleotides in an antisense RNA are required for rapid target RNA binding *in vitro* and inhibition *in vivo*. *Nucleic Acids Res* **23**, 580–587.

Kolb, F. A., Engdahl, H. M., Slagter-Jäger, J. G., Ehresmann, B., Ehresmann, C., Westhof, E., Wagner, E. G. H. & Romby, P. (2000a). Progression of a loop-loop complex to a four-way junction is crucial for the activity of a regulatory antisense RNA. *EMBO J* **19**, 5905–5915.

Kolb, F. A., Malmgren, C., Westhof, E., Ehresmann, C., Ehresmann, B., Wagner, E. G. H. & Romby, P. (2000b). An unusual structure formed by antisense-target RNA binding involves an extended kissing complex with a four-way junction and a side-by-side helical alignment. *RNA* **6**, 311–324.

Kolb, F. A., Westhof, E., Ehresmann, B., Ehresmann, C., Wagner, E. G. H. & Romby, P. (2001). Four-way junctions in antisense RNA-mRNA complexes involved in plasmid replication control: a common theme? *J Mol Biol* **309**, 605–614.

Malmgren, C., Wagner, E. G. H., Ehresmann, C., Ehresmann, B. & Romby, P. (1997). Antisense RNA control of plasmid R1 replication: the dominant product of the antisense RNA-mRNA binding is not a full RNA duplex. *J Biol Chem* **272**, 12508–12512.

Rasmussen, A. A., Eriksen, M., Gilany, K., Udesen, C., Franch, T., Petersen, C. & Valentin-Hansen, P. (2005). Regulation of *ompA* mRNA stability: the role of a small regulatory RNA in growth phase-dependent control. *Mol Microbiol* **58**, 1421–1429.

Thisted, T., Sørensen, N., Wagner, E. G. H. & Gerdes, K. (1994). Mechanism of postsegregational killing: Sok antisense RNA interacts with Hok mRNA via its 5′-end single-stranded leader and competes with the 3′-end of Hok mRNA for binding to the *mok* translational initiation region. *EMBO J* **13**, 1960–1968.

Udekwu, K. I., Darfeuille, F., Vogel, J., Reimegard, J., Holmqvist, E. & Wagner, E. G. H. (2005). Hfq-dependent regulation of OmpA synthesis is mediated by an antisense RNA. *Genes Dev* **19**, 2355–2366.

Wagner, E. G. H. & Brantl, S. (1998). Kissing and RNA stability in antisense control of plasmid replication. *Trends Biochem Sci* **23**, 451–454.

Wagner, E. G. H., Altuvia, S. & Romby, P. (2002). Antisense RNAs in bacteria and their genetic elements. In *Adv in Genetics*, pp. 361–398. Edited by J. C. Dunlap & C. Wu. London: Academic Press.

Zhang, A., Wassarman, K. M., Ortega, J., Steven, A. C. & Storz, G. (2002). The Sm-like Hfq protein increases OxyS RNA interaction with target mRNAs. *Mol Cell* **9**, 11–22.

Edited by: L. S. Frost